nature structural & molecular biology

Noncoding RNAs prevent spreading of a repressive histone mark

Claudia Keller[1,2,4], Raghavendran Kulasegaran-Shylini[1,2,4], Yukiko Shimada[1,2], Hans-Rudolf Hotz[1–3] & Marc Bühler[1,2]

Transcription of eukaryotic genomes is more widespread than was previously anticipated and results in the production of many non–protein-coding RNAs (ncRNAs) whose functional relevance is poorly understood. Here we demonstrate that ncRNAs can counteract the encroachment of heterochromatin into neighboring euchromatin. We have identified a long ncRNA (termed BORDERLINE) that prevents spreading of the HP1 protein Swi6 and histone H3 Lys9 methylation beyond the pericentromeric repeat region of *Schizosaccharomyces pombe* chromosome 1. BORDERLINE RNAs act in a sequence-independent but locus-dependent manner and are processed by Dicer into short RNAs referred to as brdrRNAs. In contrast to canonical centromeric short interfering RNAs, brdrRNAs are rarely loaded onto Argonaute. Our analyses reveal an unexpected regulatory activity of ncRNAs in demarcating an epigenetically distinct chromosomal domain that could also be operational in other eukaryotes.

In addition to synthesizing mRNAs, eukaryotic cells produce a plethora of RNAs that appear to be ncRNAs. Whereas substantial progress has been made in cataloging ncRNAs[1–3], the extent of their involvement in regulatory circuits and the mechanisms by which they might act remain to be explored further. In the fission yeast *S. pombe*, ncRNAs are known to have a prominent role in the assembly and maintenance of heterochromatin by recruiting the heterochromatin-assembly machinery to the respective genomic loci[4,5]. Transcription of pericentromeric repeat sequences at *S. pombe* centromeres results in the production of long ncRNAs (lncRNAs) that are processed by Dicer (Dcr1) into short ncRNAs (siRNAs). These are found in Argonaute (Ago1) and target the Ago1-containing RNA-induced transcriptional-silencing complex (RITS) to nascent chromatin-bound lncRNAs[6,7]. Subsequently, RITS recruits the histone methyltransferase (HMTase) Clr4, which catalyzes histone H3 Lys 9 (H3K9) methylation, a hallmark of heterochromatin[8]. Thus, long and short ncRNAs cooperate in the targeting of histone-modifying activity to appropriate locations in the *S. pombe* genome to result in higher-order chromatin states[9].

A key and conserved feature of heterochromatin is its ability to spread along chromatin from specific nucleation sites[10]. However, heterochromatin spreading is limited by DNA elements referred to as 'barriers', and this results in defined heterochromatic domains[11]. At the silent mating-type locus in *S. pombe*, the RNA interference (RNAi) machinery and transcription factors independently recruit heterochromatic factors to specific nucleation sites, from which heterochromatin subsequently spreads until it encounters barrier elements bound by the transcription-factor TFIIIC complex[5,12–15]. Heterochromatin domains at centromeres are often demarcated by clusters of tRNA genes (**Fig. 1a**)[16]. These also assemble TFIIIC and prohibit the spreading of heterochromatin[17–19]. However, it is not yet known whether productive transcription at these barrier elements is involved in antagonizing the propagation of heterochromatin. Furthermore, tRNA genes are not present on the right side of centromere 1 (cen1-R) (**Fig. 1a**), and this raises the question of how heterochromatin is restricted at this location.

HP1 proteins belong to a highly conserved family of proteins that bind methylated H3K9 with high specificity and are central to the spread of heterochromatin. In *Drosophila melanogaster*, chromatin-bound HP1 has been shown to mediate recruitment of a Clr4 homolog that methylates H3K9 on adjacent nucleosomes[20]. Similarly, the *S. pombe* HP1 homolog Swi6 is involved in heterochromatin spreading through a stepwise higher-order oligomerization process and recruitment of histone-modifying activities[5,13,21,22]. Thus, iterative HP1 binding to methylated H3K9 and recruitment of HMTase activity might be a conserved mechanism of heterochromatin spreading[23]. Notably, we discovered that Swi6 has affinity for RNA, and, when bound to RNA, it dissociates from H3K9-methylated nucleosomes[24]. Therefore, we hypothesized that RNA-mediated eviction of Swi6 from chromatin might be a mechanism counteracting heterochromatin spreading in *S. pombe*.

To gain insights into the mechanisms by which heterochromatin boundaries are established, we investigated the potential role of RNA binding to Swi6 in the demarcation of heterochromatic domains. Our genome-wide analysis of H3K9 methylation revealed that RNA binding to Swi6 is required for heterochromatin boundary formation at cen1-R. This pericentromeric heterochromatin border lacks tRNA genes, but we have identified a lncRNA, termed BORDERLINE,

[1]Friedrich Miescher Institute for Biomedical Research, Basel, Switzerland. [2]University of Basel, Basel, Switzerland. [3]Swiss Institute of Bioinformatics, Basel, Switzerland. [4]These authors contributed equally to this work. Correspondence should be addressed to M.B. (marc.buehler@fmi.ch).

Received 9 January; accepted 30 May; published online 21 July; addendum published after print 25 September 2013; doi:10.1038/nsmb.2619

that is expressed from this region and counteracts spreading of heterochromatin. BORDERLINE RNAs are processed by Dcr1 into siRNAs referred to as brdrRNAs. In contrast to canonical centromeric-repeat siRNAs, brdrRNAs are rarely loaded onto Argonaute. Notably, BORDERLINE can be replaced with a heterologous sequence without compromising boundary activity, and this demonstrates that the production of RNA is sufficient to demarcate a heterochromatic domain, irrespective of the underlying DNA sequence. Our results thus support a model in which ncRNAs produced at the heterochromatin boundary of cen1-R evict Swi6 from chromatin and thereby prevent spreading of heterochromatin into neighboring euchromatic protein-coding genes. Thus, in contrast to centromeric-repeat ncRNAs that recruit the heterochromatin-assembly machinery to chromatin, the new class of ncRNAs that we have now identified counteracts deposition of the H3K9 methyl mark outside centromeric repeats.

RESULTS

RNA binding to Swi6 demarcates heterochromatin

Swi6 consists of an N-terminal chromodomain and a structurally related C-terminal chromo shadow domain, separated by a hinge region. Stimulated by positively charged residues in the hinge region, RNA competes with methylated histone H3K9 for binding to the chromodomain of Swi6 (ref. 24). Hence, Swi6 binding to RNA is incompatible with stable heterochromatin association. If the positively charged residues in the hinge region of Swi6 are mutated to alanine (NLS-Swi6-KR25A, herein referred to as Swi6*), RNA binding but not H3K9 methyl binding is strongly impaired, and competition is no longer observed[24]. To determine whether Swi6 spreads beyond heterochromatin boundaries when it can no longer bind RNA, we performed chromatin immunoprecipitation (ChIP) experiments with cells expressing a GFP-tagged mutant form of Swi6 that does not bind

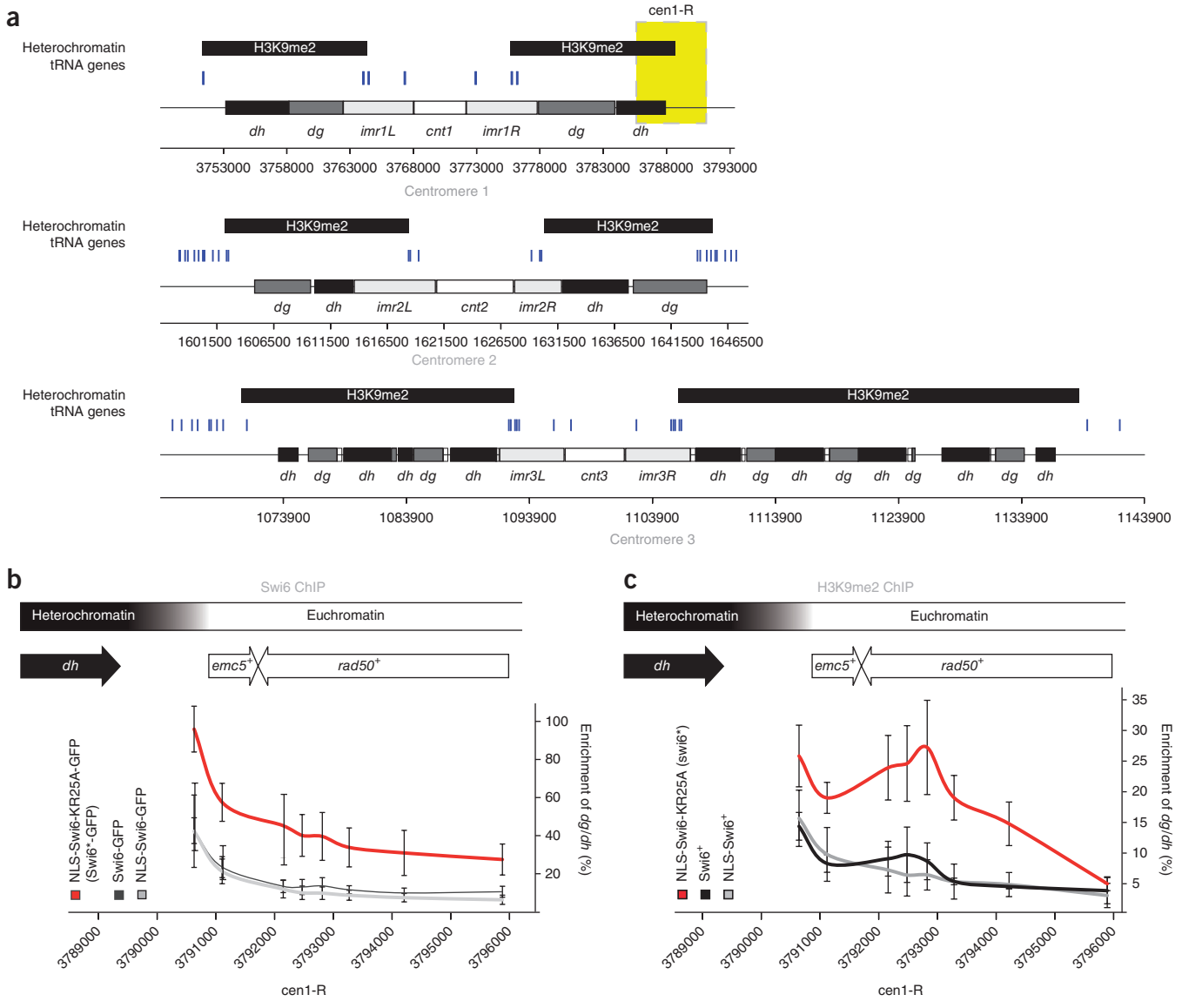

Figure 1 The ability of Swi6 to bind RNA is a factor restricting heterochromatin to pericentromeric repeats on chromosome 1. (**a**) Physical map showing the organization of the three *S. pombe* centromeres. The pericentromeric *dg* and *dh* tandem repeats are assembled into heterochromatin. *cnt*, central core domain; *imr*, innermost repeats; cen1-R, heterochromatin-euchromatin boundary region to the right of centromere 1; blue lines, tRNA genes. (**b**,**c**) ChIP-PCR experiments for Swi6 (**b**) and H3K9me2 (**c**) showing dependence of heterochromatin boundary formation at cen1-R on the RNA affinity of Swi6. Percentage DNA precipitation is shown relative to input DNA. Enrichment of H3K9me2 on *dg* and *dh* (*dg*/*dh*) repeats was set at 100% for each sample. Error bars, s.e.m.; $n \geq 3$ independent biological replicates. Nucleotide positions along chromosome are shown at bottom of each figure.

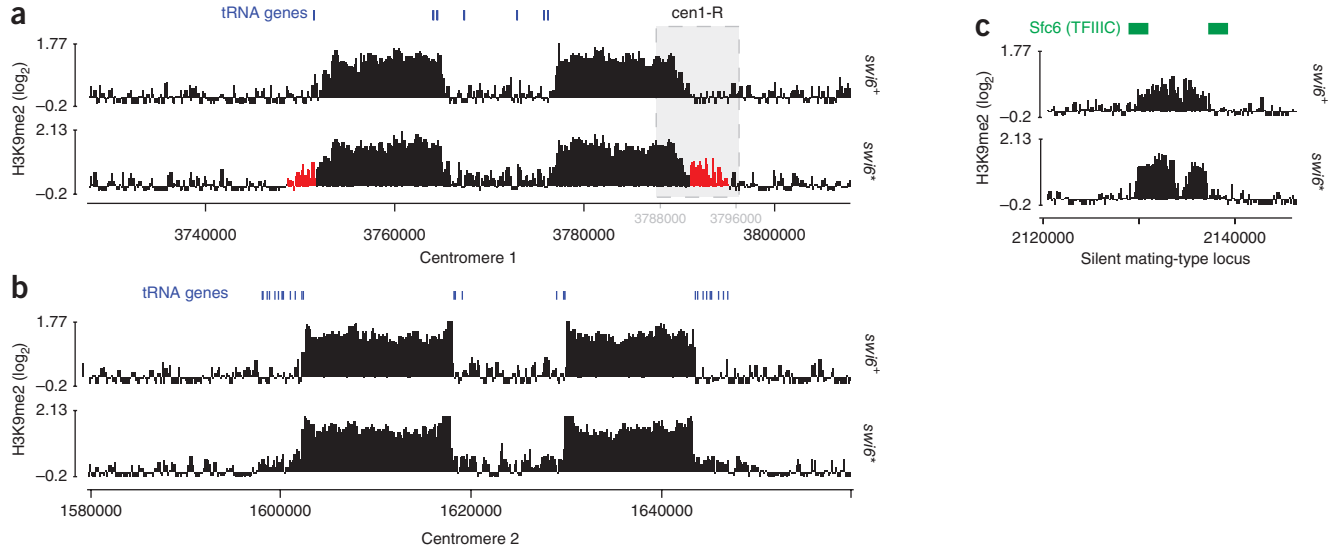

Figure 2 Spreading of heterochromatin into neighboring euchromatin in *swi6** cells occurs specifically on centromere 1 but not on centromere 2 or at the mating-type locus. (**a**) H3K9me2 ChIP-seq enrichment profiles for *swi6*$^+$ and *swi6** cells on centromere 1. The region on the right arm of chromosome 1 (cen1-R), where barrier activity is impaired in *swi6** cells, is shown in gray. (**b**) H3K9me2 ChIP-seq enrichment profiles for *swi6*$^+$ and *swi6** cells on centromere 2. **Supplementary Figure 4** shows ChIP-PCR for the same region. (**c**) Distribution of H3K9me2 at the silent mating-type locus. Green bars represent the distribution of TFIIIC (Sfc6), as determined in ref. 18. The *y* axes in **a**–**c** represent $\log_2$ ChIP-seq enrichments in 200-base-pair genomically tiled windows calculated over *clr4*Δ cells.

RNA (Swi6*-GFP) (**Supplementary Fig. 1**)[24]. Indeed, we observed spreading of Swi6*-GFP into the normally euchromatic *emc5*$^+$ and *rad50*$^+$ genes (**Fig. 1b**). Thus, the ability of Swi6 to bind RNA is a crucial factor restricting Swi6 to pericentromeric heterochromatin on chromosome 1.

To test whether heterochromatin-proximal nucleosomes become H3K9 methylated in *swi6** cells, we performed ChIP with an antibody specific to dimethyl H3K9 (H3K9me2). This revealed strongly elevated H3K9me2 levels on the *emc5*$^+$ and *rad50*$^+$ genes in *swi6** cells (**Fig. 1c**). To obtain a more comprehensive data set, we subjected the immunoprecipitated material to deep sequencing (ChIP-seq). Globally, H3K9me2 profiles of wild-type and mutant cells are well correlated (**Supplementary Fig. 2**). This is consistent with our previous results showing that RNA binding to Swi6 is dispensable for the integrity of heterochromatin[24]. It also suggests that RNA-mediated eviction of Swi6 has a minor role, if any, in preventing the formation of ectopic heterochromatin. However, the ChIP-seq data revealed encroachment of heterochromatin into the euchromatic regions flanking centromere 1 (**Fig. 2a**). Notably, spreading of the H3K9me2 mark beyond its natural boundary in *swi6** cells was most prominent on cen1-R, where no tRNA genes are encoded (**Figs. 1a** and **2a**). Spreading of H3K9me2 was less pronounced on the left of centromere 1, where a $tRNA^{Phe}$ gene is present (**Fig. 2a** and **Supplementary Fig. 3**). No prominent spreading of H3K9me2 was observed on centromeres 3 and 2 in regions where two or more tRNA genes demarcate heterochromatin or at the silent mating-type locus (**Fig. 2b**,**c** and **Supplementary Figs. 3**–**5**). However, spreading of H3K9me2 in *swi6** cells was observed on centromere 3 when tRNA genes had been deleted (**Supplementary Fig. 5**). Thus, at the mating-type locus and on centromeres 2 and 3, the barrier activity of DNA elements that assemble TFIIIC is insensitive to the disruption of RNA binding to Swi6. This suggests that productive transcription at these sites is not a prerequisite for barrier activity. Rather, barrier function might depend on the local concentration of TFIIIC. However, in the absence of TFIIIC, RNA binding to Swi6 is crucial to the restriction of heterochromatin spreading.

RNA synthesis antagonizes H3K9 methylation

The spreading of heterochromatin into cen1-R observed in *swi6** cells implies the involvement of RNA in boundary formation. Notably, an ncRNA gene (*SPNCRNA.95*) at the boundary of cen1-R heterochromatin has been annotated (**Fig. 3a**). However, northern blot analysis with probes hybridizing to the annotated sequence revealed that at least three lncRNA isoforms are produced from this region (**Fig. 3b**). Because these lncRNAs are transcribed at the border of pericentromeric heterochromatin, we named them BORDERLINE.

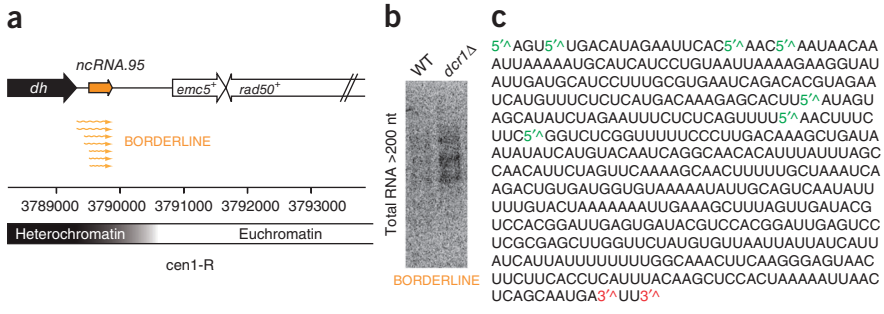

Figure 3 lncRNAs are produced at the heterochromatin boundary of cen1-R. (**a**) Physical map of the right arm of chromosome 1 indicating the heterochromatic and euchromatic regions. Orange, BORDERLINE lncRNAs. (**b**) Northern blot showing BORDERLINE lncRNAs produced from cen1-R. Strand-specific ^{32}P-labeled oligonucleotide probes were used. **Supplementary Figures 1** and **7** show the loading control and uncropped images, respectively. (**c**) Sequence of BORDERLINE as determined by RACE-PCR and Sanger sequencing. The different 5′ ends are shown in green. The 3′ ends can differ in two Us (red) and are followed by an oligo(A) tail.

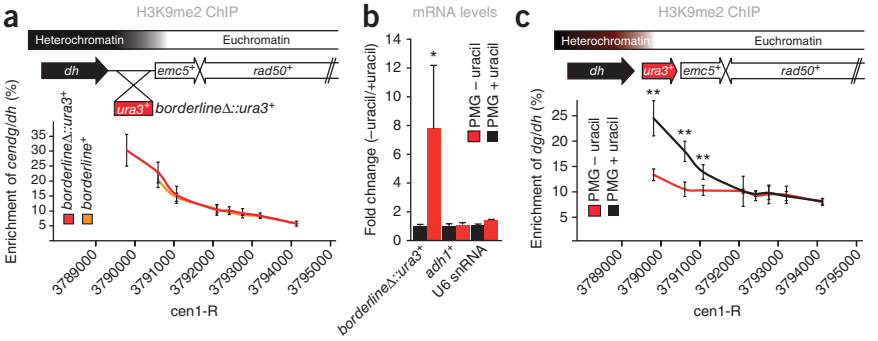

Figure 4 Production of RNA, irrespective of the underlying DNA sequence, is sufficient for heterochromatin boundary formation at cen1-R. (**a**) Spreading of H3K9me2 beyond BORDERLINE or *borderline*Δ::*ura3*$^+$, assessed by ChIP-PCR. The BORDERLINE DNA sequence was replaced with a heterologous *ura3*$^+$ expression cassette from *C. albicans* (red), for which expression is enhanced in uracil-depleted medium. Enrichments over input values normalized to *adh1*$^+$ are shown relative to enrichment of H3K9me2 on *dg* and *dh* repeats. Average fold enrichment ± s.d. is shown for at least three independent experiments. (**b**) *ura3*$^+$, *adh1*$^+$ and U6 RNA levels, determined by quantitative real-time PCR. Fold-change RNA levels are shown relative to those for cells grown in *pombe* minimal glutamate (PMG) medium with uracil and normalized to *act1*$^+$ RNA. $^*P < 0.05$. (**c**) As in **a**, with the same cell cultures from **b** used in H3K9me2 ChIP analysis. $^{**}P < 0.01$. *P* values in **a**–**c** were generated by Student's *t* test (two-tailed distribution; two-sample, unequal variance). Error bars, s.e.m. for four independent biological replicates.

Rapid amplification of cDNA ends by PCR (RACE-PCR) revealed that BORDERLINE RNAs are unidirectionally transcribed and polyadenylated. The same analysis also revealed that the isoforms share the same 3′ but not 5′ ends and that transcription starts within centromere 1 (**Fig. 3c**). Thus, transcription of BORDERLINE is initiated from several sites within centromere 1 but is terminated at a defined site.

The above results support a model in which BORDERLINE ncRNAs produced at the heterochromatin boundary of cen1-R evict Swi6 from chromatin and that this prevents spreading of heterochromatin into neighboring euchromatic protein-coding genes. As we could not rule out the possibility that this region encodes putative *cis*-acting DNA elements that recruit boundary factors, we decided to delete the BORDERLINE-encoding region and replace it with a heterologous *ura3*$^+$ expression cassette from *Candida albicans* (**Fig. 4a**). Notably, the *ura3*$^+$ transgene is about the same size as the deleted endogenous BORDERLINE-encoding region, and its expression level is defined by the concentration of uracil in the growth medium (**Fig. 4b**). Consistent with RNA-mediated heterochromatin boundary formation at cen1-R, H3K9me2 ChIP experiments revealed that replacing the BORDERLINE DNA sequence with *ura3*$^+$ was sufficient to preserve barrier activity (**Fig. 4a**,**c**). Notably, we observed an anticorrelation between H3K9me2 and *ura3*$^+$ mRNA levels, demonstrating that barrier activity increases with the amount of *ura3*$^+$ RNA produced from this locus (**Fig. 4c**). Therefore, we conclude that the underlying DNA sequence of the cen1-R boundary is not critical for boundary formation and that the mere production of RNA is enough to counteract heterochromatin spreading.

BORDERLINE RNAs are processed into small RNAs

lncRNAs produced from centromeric repeats are rapidly processed by the RNAi machinery into siRNAs that are loaded onto Ago1 (refs. 25–27). We were able to detect small RNAs by northern blotting when using probes specific for BORDERLINE in wild-type cells (**Fig. 5a**). However, these small RNAs were not detectable in *dcr1*Δ cells. Instead, we observed strongly elevated signals for BORDERLINE lncRNAs in *dcr1*Δ compared with wild-type cells (**Fig. 3b**).

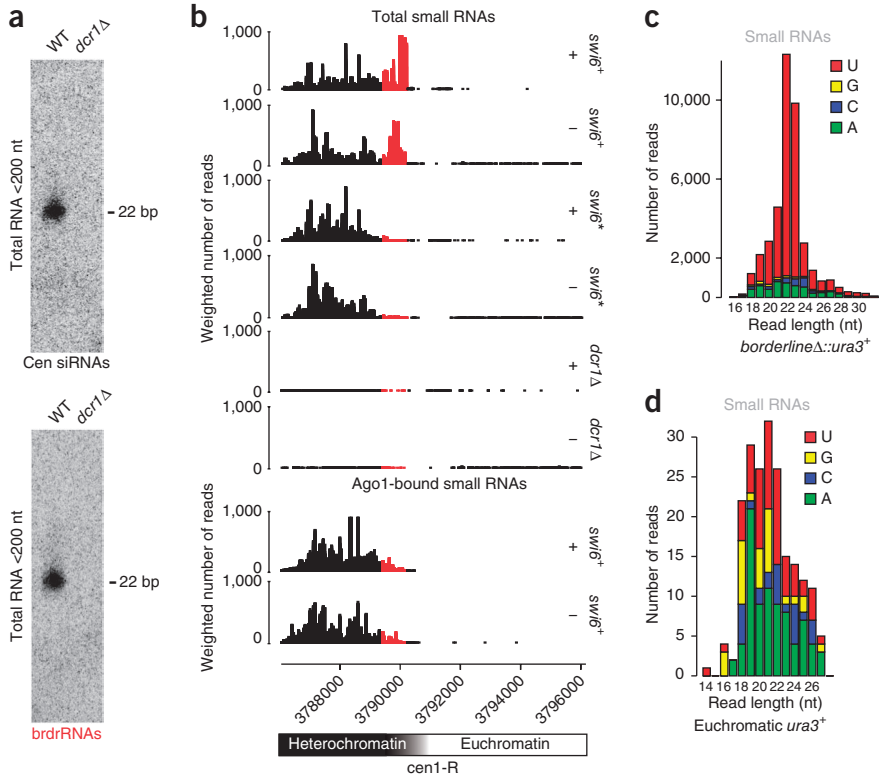

Figure 5 RNAs produced at the border of heterochromatin on centromere 1 are processed into siRNAs that fail to load onto Ago1. (**a**) Small-RNA northern blot showing siRNAs derived from centromeric-repeat lncRNAs (top, cen siRNAs) or BORDERLINE lncRNAs (bottom, brdrRNA) produced from cen1-R. Strand-specific ^{32}P-labeled oligonucleotide probes were used. Bp, base pairs. Uncropped images are shown in **Supplementary Figure 7**. (**b**) Small-RNA reads obtained by deep sequencing of total small-RNA libraries (18-nt to 28-nt PAGE-purified small RNAs) or libraries generated from Ago1-bound siRNAs[26], mapped to the cen1-R region. Red, brdrRNAs; + and – denote orientation of the RNA. **Supplementary Figure 6** shows the entire centromeric region of chromosome 1. (**c**,**d**) Small-RNA reads obtained by deep sequencing of total small-RNA libraries, mapped to the *ura3*$^+$ coding sequence. The *ura3*$^+$ gene was inserted into the *borderline*$^+$ locus (*borderline*Δ::*ura3*$^+$) or euchromatin (euchromatic *ura3*$^+$). Color code denotes nucleotides found at the 5′ end of the small-RNA reads. Nt, nucleotides.

Thus, akin to repeat RNAs, BORDERLINE lncRNAs are processed into siRNAs by Dcr1. Consistent with our northern blot analysis, deep sequencing of total small-RNA libraries revealed a prominent peak of Dcr1-dependent small-RNA reads coinciding with the left and right borders of heterochromatin on centromere 1 (**Fig. 5b** and **Supplementary Fig. 6**). Therefore, we refer to these small ncRNAs as border RNAs (brdrRNAs). Notably, *ura3*$^{+}$ mRNA was also processed into small RNAs when expressed from the cen1-R locus. These are roughly 22 nucleotides (nt) long and start with a 5′ U, which are both predictive features of true siRNAs in *S. pombe*[25] (**Fig. 5c**). In contrast, only a few reads matching the *ura3*$^{+}$ coding sequence were obtained when the *ura3*$^{+}$ gene was inserted into a euchromatic locus (**Fig. 5d**). These small-RNA reads are strand specific, show no preference for a specific 5′ nucleotide and are not length restricted; hence, we regard them as degradation products (**Fig. 5d** and **Supplementary Fig. 6**). These results demonstrate that the RNAi machinery generates brdrRNAs in a locus-dependent but sequence-independent manner.

brdrRNAs are distinct from canonical centromeric siRNAs

Accumulation of centromeric siRNAs and the methylation of H3K9 are mutually dependent processes in *S. pombe*[7,28–30]. Notably, H3K9me2 and centromeric siRNA levels are correlated within centromeric repeat sequences. This is not the case for brdrRNAs. In particular, brdrRNAs are absent from total small-RNA libraries generated from *swi6** cells, in which H3K9me2 levels are high at the cen1-R boundary (**Fig. 5b**). This raises the possibility that Swi6 is directly involved in initiating Dcr1-mediated processing of BORDERLINE transcripts. Alternatively, spreading of heterochromatin beyond cen-1R in *swi6** cells may abolish BORDERLINE transcription. We did not detect BORDERLINE transcripts in *swi6** cells (C.K., unpublished data), consistent with the latter possibility. Unexpectedly, when aligning reads obtained from deep sequencing of Ago1-associated small RNAs instead of total small-RNA libraries, we noticed a collapse of the brdrRNA peak (**Fig. 5b** and **Supplementary Fig. 6**). Thus, in contrast to centromeric siRNAs, brdrRNAs fail to load efficiently onto Ago1. This result explains why H3K9me2 levels are low despite the high number of brdrRNAs produced at cen1-R, and it raises the possibility that brdrRNAs evict Swi6 instead of guiding RITS and Clr4 to chromatin.

In summary, although both centromeric-repeat siRNAs and brdrRNAs strictly depend on Dcr1, we observed two major differences. First, repeat siRNA levels remain unaffected, but brdrRNAs are lost in *swi6** cells. Second, brdrRNAs are under-represented in small-RNA libraries generated from affinity-purified Ago1. Thus, unlike repeat siRNAs, brdrRNAs depend on the RNA affinity of Swi6, and the majority are not loaded onto Ago1.

DISCUSSION

In this work, we have identified and characterized BORDERLINE RNAs as a new class of lncRNAs that prohibit the spread of pericentromeric heterochromatin into adjacent euchromatin, most probably through eviction of Swi6 from the chromatin template. In contrast to the recurring theme that ncRNAs recruit or guide proteins to chromatin, our results indicate that RNA can also counteract chromatin association of protein factors. This is reminiscent of earlier studies revealing that mammalian lncRNAs can act as decoys, thus titrating transcription factors away from their DNA targets[31–33]. However, a distinctive feature of BORDERLINE transcripts is that they act in a sequence-independent manner, which is not the case for classical decoy-type lncRNAs. Thus, sequence conservation will not be a useful criterion to identify lncRNAs of the BORDERLINE type.

Other important features of BORDERLINE transcripts are that they function locus specifically and that they are converted into small RNAs. Thus, BORDERLINE-class lncRNAs are truly noncoding and unstable.

An unexpected finding of this study is that brdrRNAs fail to load efficiently onto Ago1, a result prompting the question of how brdrRNAs are different from centromeric siRNAs. Notably, small ncRNAs generated by Dicer proteins conventionally act as guides targeting Argonaute-containing protein complexes to their respective targets. This does not apply to the brdrRNAs identified in this study, which are rarely loaded onto Ago1 and thus cannot act as guides to target RITS to chromatin. It is possible that brdrRNAs are functionally irrelevant and simply reflect Swi6-mediated degradation of BORDERLINE transcripts through the RNAi pathway. This would be in line with Swi6 serving a general role of linking transcription to downstream RNA turnover[24,34]. Alternatively, brdrRNAs may act as repellents and evict Swi6 from chromatin. This is an attractive hypothesis because Dcr1 could then potentiate barrier activity by processing one long BORDERLINE RNA into several short brdrRNAs. Thereby, Dcr1 would guarantee a high local concentration of Swi6 evictors and hence compensate for the low transcriptional activity of the heterochromatic BORDERLINE-encoding gene. Consistent with this idea, 20-mer

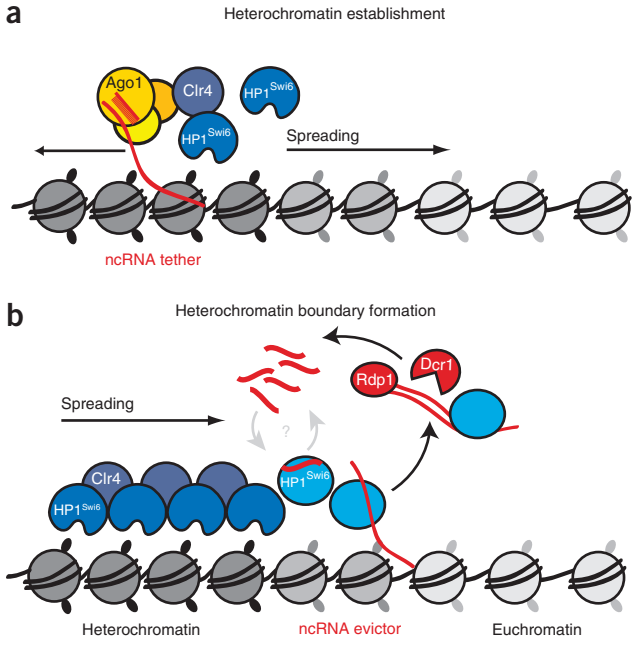

Figure 6 Involvement of opposing activities of ncRNAs in the formation of a distinct heterochromatin domain. (**a**) Chromatin-associated lncRNAs act as assembly platforms recruiting the H3K9 methyltransferase Clr4 to heterochromatin nucleation sites. Centromeric repeat–derived siRNA guide molecules that associate with the RNAi factor Ago1 provide specificity. Iterative HP1 binding to methylated H3K9 and recruitment of Clr4 results in heterochromatin spreading. This is likely to be reinforced by additional nucleation sites, thus resulting in the formation of an extended heterochromatic domain. Cotranscriptional siRNA biogenesis and direct transfer of siRNAs to Ago1 prevents unwanted Swi6 eviction within pericentromeric repeats. (**b**) Model for ncRNA function in boundary formation. BORDERLINE lncRNAs originating proximal to the centromeric repeats bind Swi6. This triggers a conformational change in the chromodomain that leads to eviction of Swi6 from chromatin and thus discontinuation of heterochromatin spreading. Subsequently, BORDERLINE lncRNAs are processed into brdrRNAs by the RNAi machinery. Unlike repeat-derived siRNAs, brdrRNAs fail to load onto Ago1. Whether brdrRNAs also participate in the eviction of Swi6 is not known.

synthetic RNA oligonucleotides bind Swi6 and are sufficient to compete with methylated H3K9 for Swi6 binding *in vitro*[24]. We could not demonstrate conclusively whether brdrRNAs bind Swi6 *in vivo*, because expression of brdrRNAs is abolished in *swi6*$^{+}$ cells. Eventually, the functional relevance of brdrRNAs in boundary formation needs to be tested genetically. Because known mutations that affect siRNA generation also disrupt heterochromatin, this is not possible at present, and this model therefore awaits definitive proof.

The involvement of the *S. pombe* RNAi pathway in the assembly of centromeric heterochromatin has been well established[9,35,36]. A key feature of RNAi-mediated heterochromatin formation is that RNAi acts cotranscriptionally and in a positive feedback loop that promotes high levels of H3K9 methylation and siRNAs. Notably, loading of centromeric siRNAs onto Ago1 is perceived as an essential step that ensures efficient Clr4 recruitment and thus maintains high H3K9 methylation levels throughout the pericentromeric repeat regions[37–39]. In light of this study, we predict that cotranscriptional processing of centromeric lncRNAs and subsequent direct transfer of siRNAs to Ago1 also prevents unwanted Swi6 eviction from centromeric repeat sequences. We are left with the question of why repeat siRNAs but not brdrRNAs are loaded onto Ago1.

Collectively, BORDERLINE and brdrRNAs constitute a class of ncRNAs that attenuate rather than assemble heterochromatin. This is in stark contrast to the well-established activity of centromeric-repeat ncRNAs in the assembly of heterochromatin. Analogously, centromere repeat–embedded but not repeat-proximal reporter genes are subject to heterochromatin formation and silencing, and they do not have barrier activity[40]. Thus, heterochromatin barrier activity of RNA is locus specific. Notably, RNA sequence is irrelevant for barrier function, a result demonstrating that BORDERLINE RNA is truly noncoding: it neither encodes a protein nor contains *cis*-acting RNA sequences that might be recognized by putative boundary factors. We propose a model in which BORDERLINE lncRNAs are processed in an RNAi-dependent manner into ~22-nt short brdrRNAs. Stimulated by positively charged residues in the hinge region, these long and/or small ncRNAs compete with methylated histone H3K9 for binding to the chromodomain of Swi6. Consequently, this causes Swi6 eviction from chromatin, which counteracts the spreading of heterochromatin (**Fig. 6**). Considering the high conservation of HP1 proteins and the production of ncRNAs from silent chromatin in higher eukaryotes, we anticipate that similar mechanisms shaping the epigenome also operate in other organisms.

METHODS

Methods and any associated references are available in the online version of the paper.

Accession code. ChIP-seq and small RNA sequencing data have been submitted to the Gene Expression Omnibus under accession number GSE42850.

Note: Supplementary information is available in the online version of the paper.

ACKNOWLEDGMENTS

We are grateful to T. Roloff, K. Jacobeit, S. Dessus-Babus and D. Gaidatzis for help with Illumina deep sequencing, data processing and data analysis. This work was supported by funds to M.B. from the Swiss National Science Foundation (PP00P3_139204/1), the European Research Council (280410) and the European Molecular Biology Organization Young Investigator Programme (922.001). R.K.-S. was supported by a postdoctoral fellowship from the Peter and Traudl Engelhorn Foundation. The Friedrich Miescher Institute for Biomedical Research is supported by the Novartis Research Foundation.

AUTHOR CONTRIBUTIONS

R.K.-S., C.K. and Y.S. performed ChIP experiments. R.K.-S. prepared libraries for ChIP-seq and analyzed the data and performed RACE experiments. C.K. created strains, performed Northern blotting and quantitative real-time PCR and prepared RNA for small-RNA deep sequencing. H.-R.H. conducted bioinformatic analysis of small-RNA deep-sequencing data. M.B., C.K. and R.K.-S. designed the study, analyzed the data and wrote the manuscript.

COMPETING FINANCIAL INTERESTS

The authors declare no competing financial interests.

1. Djebali, S. *et al.* Landscape of transcription in human cells. *Nature* **489**, 101–108 (2012).
2. Wilhelm, B.T. *et al.* Dynamic repertoire of a eukaryotic transcriptome surveyed at single-nucleotide resolution. *Nature* **453**, 1239–1243 (2008).
3. Nagalakshmi, U. *et al.* The transcriptional landscape of the yeast genome defined by RNA sequencing. *Science* **320**, 1344–1349 (2008).
4. Volpe, T.A. *et al.* Regulation of heterochromatic silencing and histone H3 lysine-9 methylation by RNAi. *Science* **297**, 1833–1837 (2002).
5. Hall, I.M. *et al.* Establishment and maintenance of a heterochromatin domain. *Science* **297**, 2232–2237 (2002).
6. Verdel, A. *et al.* RNAi-mediated targeting of heterochromatin by the RITS complex. *Science* **303**, 672–676 (2004).
7. Motamedi, M.R. *et al.* Two RNAi complexes, RITS and RDRC, physically interact and localize to noncoding centromeric RNAs. *Cell* **119**, 789–802 (2004).
8. Bayne, E.H. *et al.* Stc1: a critical link between RNAi and chromatin modification required for heterochromatin integrity. *Cell* **140**, 666–677 (2010).
9. Lejeune, E. & Allshire, R.C. Common ground: small RNA programming and chromatin modifications. *Curr. Opin. Cell Biol.* **23**, 258–265 (2011).
10. Grewal, S.I. & Moazed, D. Heterochromatin and epigenetic control of gene expression. *Science* **301**, 798–802 (2003).
11. Sun, F.L. & Elgin, S.C. Putting boundaries on silence. *Cell* **99**, 459–462 (1999).
12. Jia, S., Noma, K. & Grewal, S.I. RNAi-independent heterochromatin nucleation by the stress-activated ATF/CREB family proteins. *Science* **304**, 1971–1976 (2004).
13. Yamada, T., Fischle, W., Sugiyama, T., Allis, C.D. & Grewal, S.I. The nucleation and maintenance of heterochromatin by a histone deacetylase in fission yeast. *Mol. Cell* **20**, 173–185 (2005).
14. Noma, K., Allis, C.D. & Grewal, S.I. Transitions in distinct histone H3 methylation patterns at the heterochromatin domain boundaries. *Science* **293**, 1150–1155 (2001).
15. Thon, G., Bjerling, P., Bunner, C.M. & Verhein-Hansen, J. Expression-state boundaries in the mating-type region of fission yeast. *Genetics* **161**, 611–622 (2002).
16. Wood, V. *et al.* The genome sequence of *Schizosaccharomyces pombe*. *Nature* **415**, 871–880 (2002).
17. Scott, K.C., Merrett, S.L. & Willard, H.F. A heterochromatin barrier partitions the fission yeast centromere into discrete chromatin domains. *Curr. Biol.* **16**, 119–129 (2006).
18. Noma, K., Cam, H.P., Maraia, R.J. & Grewal, S.I. A role for TFIIIC transcription factor complex in genome organization. *Cell* **125**, 859–872 (2006).
19. Scott, K.C., White, C.V. & Willard, H.F. An RNA polymerase III-dependent heterochromatin barrier at fission yeast centromere 1. *PLoS ONE* **2**, e1099 (2007).
20. Schotta, G. *et al.* Central role of *Drosophila* SU(VAR)3–9 in histone H3–K9 methylation and heterochromatic gene silencing. *EMBO J.* **21**, 1121–1131 (2002).
21. Canzio, D. *et al.* Chromodomain-mediated oligomerization of HP1 suggests a nucleosome-bridging mechanism for heterochromatin assembly. *Mol. Cell* **41**, 67–81 (2011).
22. Nakayama, J., Rice, J.C., Strahl, B.D., Allis, C.D. & Grewal, S.I. Role of histone H3 lysine 9 methylation in epigenetic control of heterochromatin assembly. *Science* **292**, 110–113 (2001).
23. Grewal, S.I. & Jia, S. Heterochromatin revisited. *Nat. Rev. Genet.* **8**, 35–46 (2007).
24. Keller, C. *et al.* HP1(Swi6) mediates the recognition and destruction of heterochromatic RNA transcripts. *Mol. Cell* **47**, 215–227 (2012).
25. Bühler, M., Spies, N., Bartel, D.P. & Moazed, D. TRAMP-mediated RNA surveillance prevents spurious entry of RNAs into the *Schizosaccharomyces pombe* siRNA pathway. *Nat. Struct. Mol. Biol.* **15**, 1015–1023 (2008).
26. Halic, M. & Moazed, D. Dicer-independent primal RNAs trigger RNAi and heterochromatin formation. *Cell* **140**, 504–516 (2010).
27. Reinhart, B.J. & Bartel, D.P. Small RNAs correspond to centromere heterochromatic repeats. *Science* **297**, 1831 (2002).
28. Cam, H.P. *et al.* Comprehensive analysis of heterochromatin- and RNAi-mediated epigenetic control of the fission yeast genome. *Nat. Genet.* **37**, 809–819 (2005).

29. Noma, K. *et al.* RITS acts in *cis* to promote RNA interference-mediated transcriptional and post-transcriptional silencing. *Nat. Genet.* **36**, 1174–1180 (2004).
30. Hong, E.-J.E., Villén, J., Gerace, E.L., Gygi, S.P. & Moazed, D. A Cullin E3 ubiquitin ligase complex associates with Rik1 and the Clr4 histone H3–K9 methyltransferase and is required for RNAi-mediated heterochromatin formation. *RNA Biol.* **2**, 106–111 (2005).
31. Kino, T., Hurt, D.E., Ichijo, T., Nader, N. & Chrousos, G.P. Noncoding RNA gas5 is a growth arrest- and starvation-associated repressor of the glucocorticoid receptor. *Sci. Signal.* **3**, ra8 (2010).
32. Ng, S.Y., Johnson, R. & Stanton, L.W. Human long non-coding RNAs promote pluripotency and neuronal differentiation by association with chromatin modifiers and transcription factors. *EMBO J.* **31**, 522–533 (2012).
33. Martianov, I., Ramadass, A., Serra Barros, A., Chow, N. & Akoulitchev, A. Repression of the human dihydrofolate reductase gene by a non-coding interfering transcript. *Nature* **445**, 666–670 (2007).
34. Bühler, M. & Hiller, S. Dynamic nature of heterochromatin highlighted by a HP1 (Swi6)-dependent gene silencing mechanism. *Cell Cycle* **11**, 3907–3908 (2012).
35. Moazed, D. Small RNAs in transcriptional gene silencing and genome defence. *Nature* **457**, 413–420 (2009).
36. Grewal, S.I. & Elgin, S.C. Transcription and RNA interference in the formation of heterochromatin. *Nature* **447**, 399–406 (2007).
37. Bühler, M. & Moazed, D. Transcription and RNAi in heterochromatic gene silencing. *Nat. Struct. Mol. Biol.* **14**, 1041–1048 (2007).
38. Castel, S.E. & Martienssen, R.A. RNA interference in the nucleus: roles for small RNAs in transcription, epigenetics and beyond. *Nat. Rev. Genet.* **14**, 100–112 (2013).
39. Partridge, J.F. Centromeric chromatin in fission yeast. *Front. Biosci.* **13**, 3896–3905 (2008).
40. Allshire, R.C., Nimmo, E.R., Ekwall, K., Javerzat, J.P. & Cranston, G. Mutations derepressing silent centromeric domains in fission yeast disrupt chromosome segregation. *Genes Dev.* **9**, 218–233 (1995).

ONLINE METHODS

Strains and plasmids. Fission-yeast strains were grown at 30 °C in YES, PMG or PMG – uracil. All strains were constructed with a PCR-based protocol[41] or by standard mating and sporulation. A *ura3*$^{+}$ expression cassette from *C. albicans*[42] was used to replace the BORDERLINE-encoding DNA fragment (ChrI::3789421-3790520) on the right side of centromere 1. The C-terminally EGFP-tagged strains were created with pFA6a-link vectors[43]. All strains were confirmed by sequencing. Plasmid sequences and detailed maps are available upon request. DNA oligo sequences and strains used in this study are listed in **Supplementary Tables 1** and **2**.

Quantitative PCR. Real-time PCR was performed as described previously[44] on a Bio-Rad CFX96 Real-Time System using SsoAdvanced SYBR Green Supermix (Bio-Rad). Primer sequences are given in **Supplementary Table 1**.

Western blot. Western blotting was performed as described previously[44]. Uncropped blots are shown in **Supplementary Figure 7**.

Chromatin immunoprecipitation (ChIP). HP1^{Swi6} ChIP experiments were performed with cells expressing GFP-tagged HP1^{Swi6} protein that was fully functional (**Supplementary Fig. 1**). The anti-GFP antibody was purchased from Invitrogen (anti-GFP, rabbit IgG fraction; A11122). H3K9me2 ChIP experiments were performed with an H3K9me2-specific mouse monoclonal antibody from Wako (clone no. MABI0307; 302-32369). Anti-H3K9me antibody or anti-GFP antibody were used at 1 µg per mg of whole cell extract (WCE). Cells were processed for ChIP analysis as described previously[44], with minor modifications. Briefly, *S. pombe* cells were fixed with 1% formaldehyde for 15 min and then lysed in buffer containing 50 mM HEPES/KOH, pH 7.5, 140 mM NaCl, 1 mM EDTA, 1% Triton X-100, 0.1% Na deoxycholate, 1 mM PMSF and protease-inhibitor cocktail. Chromatin was sheared with a Bioruptor (Diagenode) to yield DNA fragments of 300–500 bp. For ChIP-seq, chromatin was sheared with a S220 Focused Ultrasonicator (Covaris), yielding DNA fragments of ~150 bp.

ChIP-sequencing. ChIP-seq libraries were generated with an Illumina-based protocol with custom reagents and bar-coded adapters. Briefly, immunoprecipitated DNA was end-repaired with a combination of T4 DNA polymerase, *E. coli* DNA Pol I large fragment (Klenow polymerase) and T4 polynucleotide kinase. The blunt phosphorylated ends were treated with Klenow fragment (32 to 52 exo minus) and dATP to yield a protruding A for ligation of Illumina adapters, which have a single T base overhang at the 3′ end. After adaptor ligation, DNA fragments were size-selected to remove excess adapters, and adaptor-modified DNA fragments were enriched by PCR amplification with Illumina primers for 18 cycles. Library fragments of ~250 bp (insert plus adaptor and PCR primer sequences) were band-isolated from an agarose gel. The purified ChIP-seq libraries thus generated were validated and subsequently captured on an Illumina flow cell for cluster generation. Libraries were sequenced on the Illumina HiSeq2000 system according to the manufacturer's protocols.

ChIP-seq reads were mapped with Bowtie version 0.9.9.1 (ref. 45) with parameters v 2 -a -m 100, tracking up to 100 best alignments for every query read. Each alignment was weighted by the inverse of the number of hits. All quantifications were based on weighted alignments. Wiggle contrast tracks were created as follows: each library was normalized for the total number of mapped reads and quantified in genomically tiled windows with a size of 200 bp. Before conversion of the data to $\log_2$ space, a pseudocount of 8 was added to each window to eliminate large changes caused by small read counts. Contrasts between samples were calculated by subtraction of the resulting values in $\log_2$ space.

Northern blot. Northern blot analysis was performed as described previously[46]. Briefly, total RNA was isolated from exponentially growing cells with the hot phenol method[47]. The RNA was fractionated with RNeasy Midi columns (Qiagen) according to the RNA cleanup protocol provided by the manufacturer. The flow-through fraction was precipitated ('small-RNA' fraction). The RNA retained on the column was eluted and ethanol-precipitated ('large-RNA' fraction), and 25 µg of the small-RNA fraction was separated by 17.5% PAGE followed by northern blotting as described previously[46]. Aliquots (50 µg) of the large-RNA fraction were separated on a 1.2% agarose gel (1× MOPS and 1% formaldehyde) and transferred to positively charged nylon membranes (Roche) by standard capillary blotting. RNAs were detected with [^{32}P]ATP-labeled oligos (**Supplementary Table 1**). Uncropped blots are shown in **Supplementary Figure 7**.

Small-RNA sequencing. Aliquots (25 µg) of the small-RNA fraction (described above) were separated by 17.5% PAGE and the 18-nt to 28-nt population purified. Libraries were prepared with the Illumina TruSeq small-RNA preparation protocol (cat. no. RS-930-1012). The 145-nt to 160-nt population was isolated and the library sequenced on an Illumina HiSeq2000. Small-RNA reads were aligned as described previously[48] with zero mismatch allowed.

Rapid amplification of cDNA ends. RACE was performed with a Clontech SMARTer RACE cDNA Amplification Kit (cat. no. 634923). First-strand synthesis and RT template encoding RACE-ready cDNAs were generated per the manufacturer's instructions. Gene-specific primers for the region of interest and universal primers for the ends were used to generate/amplify 5′ and 3′ RACE fragments.

41. Bähler, J. *et al.* Heterologous modules for efficient and versatile PCR-based gene targeting in *Schizosaccharomyces pombe*. *Yeast* **14**, 943–951 (1998).
42. Goldstein, A.L., Pan, X. & McCusker, J.H. Heterologous URA3MX cassettes for gene replacement in *Saccharomyces cerevisiae*. *Yeast* **15**, 507–511 (1999).
43. Sheff, M.A. & Thorn, K.S. Optimized cassettes for fluorescent protein tagging in *Saccharomyces cerevisiae*. *Yeast* **21**, 661–670 (2004).
44. Keller, C. *et al.* HP1(Swi6) mediates the recognition and destruction of heterochromatic rna transcripts. *Mol. Cell* **47**, 215–227 (2012).
45. Langmead, B., Trapnell, C., Pop, M. & Salzberg, S.L. Ultrafast and memory-efficient alignment of short DNA sequences to the human genome. *Genome Biol.* **10**, R25 (2009).
46. Bühler, M., Verdel, A. & Moazed, D. Tethering RITS to a nascent transcript initiates rnai- and heterochromatin-dependent gene silencing. *Cell* **125**, 873–886 (2006).
47. Leeds, P., Peltz, S.W., Jacobson, A. & Culbertson, M.R. The product of the yeast *UPF1* gene is required for rapid turnover of mRNAs containing a premature translational termination codon. *Genes Dev.* **5**, 2303–2314 (1991).
48. Emmerth, S. *et al.* Nuclear retention of fission yeast dicer is a prerequisite for RNAi-mediated heterochromatin assembly. *Dev. Cell* **18**, 102–113 (2010).

Addendum: Noncoding RNAs prevent spreading of a repressive histone mark

Claudia Keller, Raghavendran Kulasegaran-Shylini, Yukiko Shimada, Hans-Rudolf Hotz & Marc Bühler

Nat. Struct. Mol. Biol. **20, 994–1000 (2013); published online 21 July 2013; addendum published after print 25 September 2013**

It was brought to our attention that the DNA sequence that was annotated as SPNCRNA.95 in PomBase (http://www.pombase.org/) is the same as a genomic element referred to as IRC1-R in Cam *et al.*, *Nat. Genet.* **37**, 809–819, 2005. Therefore, the BORDERLINE-encoding sequence and the IRC1-R element do partially overlap (**Fig. 1**). Correct annotations and coordinates have been updated in PomBase accordingly.

We note that, when Swi6 is overexpressed, the IRC1 DNA sequence is required to stop heterochromatin spreading on the left side of centromere 1 (IRC1-L; Noma *et al.*, *Cell* **125**, 859–872, 2006), but it remains to be investigated whether the same applies to the cen1-R boundary when IRC1-R is deleted and Swi6 overexpressed. Because heterochromatin spreading in our paper was assessed under normal Swi6 expression levels, we conclude that noncoding RNA (ncRNA)–mediated boundary activity is sufficient to stop the spread of heterochromatin under physiological conditions, although overlapping or complementary mechanisms may exist.

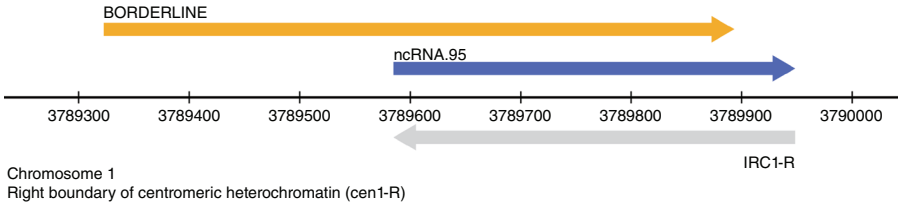

Figure 1 Schematics of BORDERLINE and ncRNA.95. Genomic locations of BORDERLINE (yellow) and ncRNA.95 (blue) on *Schizosaccharomyces pombe* chromosome 1, showing partial overlap of the elements. The sequence of the ncRNA.95 is the same as that of IRC1-R (gray).